

# Structural, Transport and magnetic Properties of $\text{Ca}_2\text{Zn}_2\text{Fe}_{12}\text{O}_{22}$ Hexagonal Y-Ferrites

C. P. Chaudhari

Department of Physics, Govt. Science College, Gadchiroli, India

Email: [shekhark8040@gmail.com](mailto:shekhark8040@gmail.com)

## Abstract-

Calcium hexagonal ferrites doped  $\text{Ca}_2\text{Zn}_2\text{Fe}_{12}\text{O}_{22}$  was prepared by solid state diffusion technique. The structural properties of this polycrystalline sample were studied using powder X-ray diffraction method. The XRD pattern showed a single phase of the Y type hexagonal ferrite with lattice parameters  $a=5.93 \text{ \AA}$  and  $c=41.32 \text{ \AA}$ . The two electrode method was used to study the DC Resistivity of the ferrite between the temperatures from 300 K to 800 K. The resistivity result showed the behaviour of samples as semiconductor. Variation in molar susceptibility of the hexagonal ferrite between temperatures 300 K to 800 K was studied by Gouy's balance method. This showed the ferrimagnetic behaviour of the sample at room temperature. Its Curie Temperature was found to be 400 K and Curie molar constant was 52.5

**Keywords:** Hexagonal ferrites, Solid state diffusion, DC resistivity, Ca- Y ferrite.

## I. INTRODUCTION

The basic crystallographic and magnetic properties of the main hexagonal ferrites have been reviewed by J. Smit and H.P.J. Wijn [1]. Hexagonal ferrites are classified on the basis of their chemical composition and crystal structure into six types: M, W, X, Y, Z, and U. It is possible to synthesise a ferrite of specific properties by controlling the chemical composition and nature of substituting element [2]. The hexagonal ferrites can be prepared by solid state diffusion technique, firing stoichiometric amounts of oxides MO (M=Ba, Sr, Pb, Ca etc),  $\text{Fe}_2\text{O}_3$  and MeO (Me=Zn, Mg, Mn, Co etc, the divalent metal ions). This method is most convenient and simple for the preparation of polycrystalline ferrites of high purity. In this method the formation of compounds depends on many factors such as particle size of reactants, sintering temperature and atmosphere [3]. The crystalline and Magnetic structures of the different types of hexagonal ferrites are remarkably complex and can be considered as a superposition of fundamental structural blocks: S, R and T blocks. The S block having spinel structure is a result of cubic close packing of two oxygen layers ( $\text{O}_4\text{-O}_4$ ) with composition  $\text{Fe}_6\text{O}_8$ . The R and T blocks result from an hexagonal close packing of oxygen layers: R block from three oxygen layers ( $\text{O}_4\text{-BaO}_3\text{-O}_4$ ) and the T block from four oxygen layers ( $\text{O}_4\text{-BaO}_3\text{-BaO}_3\text{-O}_4$ ) respectively, with part of the oxygen substituted by Ba, Sr, Ca etc. The metallic cations Me are distributed among several lattice sites different from the crystallographic and the magnetic point of view and

therefore play important role in determining the magnetic properties of the hexagonal ferrites [4]. The Y-type hexagonal ferrites have a crystalline structure built up as a superposition of S and T blocks. The unit cell is composed of the sequence STSTST including three formula units. Gorter [5] made the first attempt to determine the position of the magnetic ions and orientation of the spins in the crystal lattice by considering exchange interactions. The metallic cations are distributed among six sublattices as two tetrahedral and four octahedral sublattices. The distribution of  $\text{Zn}^{2+}$  and  $\text{Fe}^{2+}$  between the blocks is described by parameter  $\gamma$ : S block contains  $\gamma$  of  $\text{Zn}^{2+}$  ions and  $(1-\gamma)$  of  $\text{Fe}^{2+}$  ions, while the opposite holds for the T block [6]. It is worth noting that inside the T block, three octahedral ions, belonging to  $6c_{VI}$  and  $3b_{VI}$  sublattices, lies on a vertical 3-fold axis, the central  $3b_{VI}$  ion sharing two faces of its coordination figure with the adjacent  $6c_{VI}$  ions. Such a configuration is responsible for a higher potential energy of the structure due to a stronger electrostatic repulsion between the cations. Such sites are likely to be preferred by low charge ions. As a consequence non-magnetic  $\text{Me}^{2+}$  ions with a marked preference for the octahedral coordination may cause drastic changes in the magnetic configuration with respect to the usual Gorter [5] scheme; indeed the occupation of either  $6c_{VI}$  and  $3b_{VI}$  by non-magnetic ions leads to the cancellation of the antiferromagnetic  $b_{VI}\text{-}c_{IV}^*$  interaction which is the strongest one in the Y-structure. The substitution of  $\text{Ba}^{2+}$  ion by other divalent cations (i.e.  $\text{Ca}^{2+}$  ions in the present case) does not affect the site distribution [7]. The hexagonal ferrites are largely used in electronic communication, microwave devices [8], magneto-optic recording media [9], transformer cores and high quality filters due to their versatile magnetic properties [10-14]. Y-type ferrites attracted large interest in recent years due to the observation of magneto-electric effects.

## II. EXPERIMENTAL PROCEDURE

### A. Powder Preparation

The single phase polycrystalline sample of hexagonal ferrite with formula  $\text{Ca}_2\text{Zn}_2\text{Fe}_{12}\text{O}_{22}$  were synthesized by solid state diffusion technique. Analar grade powders of CaO, ZnO, and  $\text{Fe}_2\text{O}_3$  are first dried separately at  $150 \text{ }^\circ\text{C}$  for about an hour to remove the traces of moisture and are mixed intimately in 1:1:3 proportions. The powdered mixture of the oxides is ground using A.R. grade acetone in an agate mortar for about 4 hours. To obtain the particle size less than 50

micron, the sieve with 50 micron filter size was used to filter the grounded mixture. The larger size particles are again grounded until their size becomes less than 50 micron. It is known that finer the particle, swifter is the formation [15]. After grinding the mixture, it was dried in air. The powder was then mixed separately with 5% polyvinyl acetate (PVA) in A.R. grade acetone as binder (16). About 2 ml of binder per gram of the powder is found to give well-moulded pellets (17). The sample was then pressed in a stainless steel die using hydraulic press under uniaxial pressure of 5 tonne/sq. inch for 5 min to form the pellets of 15 mm in diameter and about 4-7 mm in thickness using. The pellets thus formed are heated at 300°C for about 4 hours to remove the binder. The samples were then heated at 1100°C for 120 hours so that ceramic product is obtained. Finally the temperature of the furnace is cooled down at the rate of 50°C per hour up to 500°C and then cooled down in natural way. The product masses thus formed are taken out and finely grounded for about half an hour in the agate mortar. After drying in air the powder was ready for experimental investigations [18].

### B. Pellet preparation

For electrical conductivity measurements again the pellet was prepared from powder sample. The end faces of the pellet were gently ground under distilled water. The moisture of the pellet was removed by oven heating. This is necessary because surface layer formed during firing may present difficulties. This layer can have higher resistivity than the bulk, owing to re-oxidation, particularly at the surface of the pellet during cooling, or lower resistivity than the bulk as found with mixed Ni-Zn ferrites of spinel structure [19]. A Thin layer of silver paste is applied on the both the flat surfaces of the pellet to provide good electrical contacts [20]. The contacts are dried by heating the pellet slowly at 300°C for 5 hours.

### C. Characterization

The crystalline phase determination of the sample was carried out on Philips Holand XRD unit (PW 1710) operating at 42.5 KV and 18.00 mA with filtered Cu K<sub>α</sub> radiation with wavelength 1.5405 Å. The 2θ Bragg angles were scanned over a range of 20° to 100° with a step of 0.02° for 1 second. XRD pattern was subjected to Debye Scherrer technique for checking and identifying the material. The electrical conductivity of Zn, Ca-Y ferrite was measured from 300 K to 800 K using two electrodes. A small variation in temperature 2°C per minute is maintained throughout the experiment. Magnetic susceptibility of the samples was measured from 300 K to 800 K by Gouy's method [21]. Other magnetic

properties like coercivity, retentivity and saturation magnetization were found using hysteresis loop tracer HLT-III, made by Scientific Equipments, Roorkee.

## III. RESULT AND DISCUSSION

### A. XRD analysis

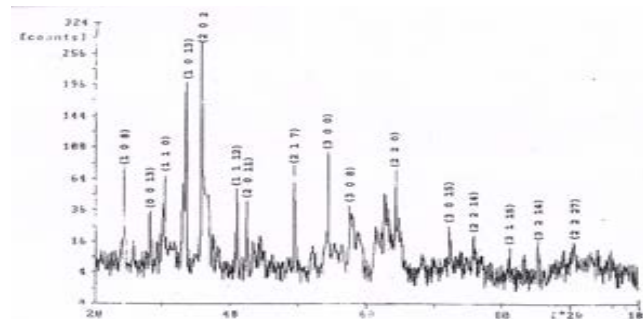


Fig: 1 X-ray diffraction pattern of Ca<sub>2</sub>Zn<sub>2</sub>Fe<sub>12</sub>O<sub>22</sub>

The XRD pattern is shown in Fig. 1. This pattern is matched with the standard pattern which is best fitted with the hexagonal ferrite and no extra lines were detected. This showed a single phase of the Y type hexagonal ferrite with lattice parameters a=5.93 Å and c=41.32 Å. These are in agreement with findings of *Kohn and Eckart* [22], that “all the rhombohedral and hexagonal ferrites are having the same basal plane (5.90 Å) but differing by the ‘c’ axis stacking of specific blocks”. The reported value of ‘c’ in Ba-Y ferrite is 43.56 Å [23] which is less as compared to observed ‘c’ in Ca-Y ferrite in the present case. The reason can be given as follows. The length ‘c’ depends on the distance between two layers of oxygen, which is the largest ion of all the ions constituting Ca-Y ferrite. The substituting metal ions occupy the interstitial positions between the two oxygen layers and the size of metal ions as well as of Ca<sup>2+</sup> ions are so small that it cannot affect the distance between two oxygen layers. But in Ba-Y ferrite barium ions are somewhat larger than oxygen ions which result in increase in distance between the two adjacent oxygen layers from 2.32 Å to 2.40 Å [24]. These parameters lead to the rhombohedral rather than hexagonal crystal structure with a space group  $R\bar{3}m$ . Since rhombohedral cell may be referred to a hexagonal cell, the compound is indexed with reference to hexagonal axes.

### B. Transport properties

Fig. 2 shows the graph of log of electrical resistivity versus temperature ( $\frac{10^3}{T}$ ). The dc electrical resistivity ( $\rho$ ) measurements were carried out by two-electrode method. The graph of log  $\rho$  versus inverse absolute temperature is shown in

Figure 4. It is observed that the slope of the log  $\rho$  versus inverse absolute temperature curve changes at the Curie point

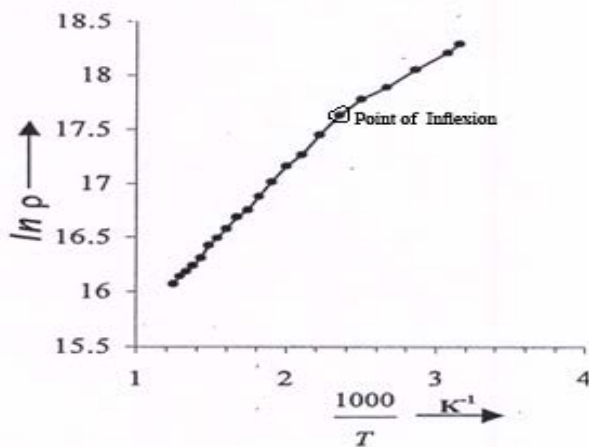


Fig: 2 graph of log of DC electrical resistivity versus inverse absolute temperature ( $\frac{1000}{T}$ ) of  $\text{Ca}_2\text{Zn}_2\text{Fe}_{12}\text{O}_{22}$

(point of inflexion) 408 K. This strongly supports the influence of magnetic ordering up on the conductivity process in ferrites. Thus, gave two different values of activation energy. It is smaller (0.150eV) in ferromagnetic region as compared above  $T_c$ , the paramagnetic region (0.28 eV). It is due to the migration of intrinsic electron between iron ions on octahedral sites within the spinel blocks [25]. The values indicate the semiconducting nature of the compound.

### C. Magnetic properties

1) *Curie temperature ( $T_c$ ):* The transition point between magnetic states was observed by Gouy's balance [21]. The ferrimagnetic sample was found to be paramagnetic above 400 K. The low value of  $T_c$  as compared to other Y-ferrite [24] accounts for the less thermal stability of the compound. The graph of inverse molar susceptibility ( $1/\chi_M$ ) versus absolute temperature is shown in Figure 3. It is linear above Curie temperature showing paramagnetic behaviour. The Curie molar constant comes out to be 52.45, close to theoretical value (52.5).

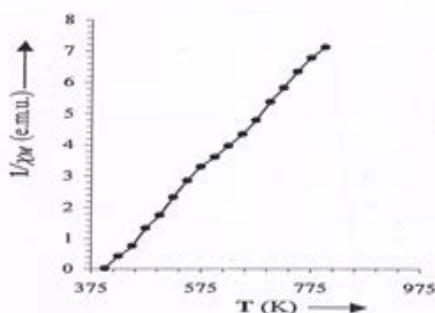


Fig. 3: Variation of inverse molar susceptibility versus absolute temperature of  $\text{Ca}_2\text{Zn}_2\text{Fe}_{12}\text{O}_{22}$

2) *Hysteresis loop properties:* Hysteresis loop is shown in Figure 4. From loop saturation magnetization ( $\sigma_s$ ), coercivity ( $H_c$ ) and effective number of Bohr magneton ( $\eta_B$ ) were calculated and found to be  $\sigma_s = 49$  gauss-cc/gm,  $H_c = 61$  Oe and  $\eta_B = 11$ . High value of saturation magnetization is due to the presence of Zn ions in tetrahedral sites of both S and T blocks so that the parallel orientation of the moments in octahedral sites is favoured. The low value of coercivity (below 200 Oe) classifies the compound as soft magnetic material [26]. Because of nonrectangular shape of loop (low  $H_c$  value), hysteresis loss is less and therefore this ferrite may be used for the low core loss requirements.

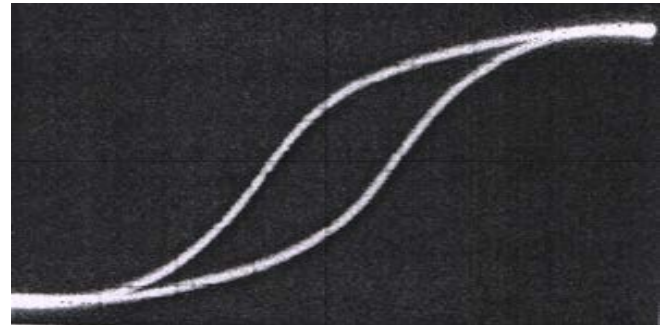


Fig. 4: Hysteresis loop for  $\text{Ca}_2\text{Zn}_2\text{Fe}_{12}\text{O}_{22}$  for magnetic field of 300 Gauss between poles of electromagnet and CRO set for 50 mV/div.

### IV. CONCLUSION

Zn substituted Ca-Y hexagonal ferrite was prepared by solid state diffusion technique. No deformation in structure is observed for  $\text{Ca}^{2+}$  cations, which replaced the larger barium ions in Ba-Y ferrite except slight reduction in 'c'. The presence of zinc weakens the superexchange interaction which in effect lowers the Curie temperature. Zinc enhances the saturation magnetization making it useful in high resonance frequency applications. Due to non-rectangular trace of hysteresis the compound may not be useful as permanent magnet. The sample is a semiconductor having two activation energies.

- [1] Smit J and Wijn, H.P.J., *Ferrites* Philips Technical Library, Eindhoven
- [2] X. Wang, D. Li. *J. Alloys. Compd.* 273 (1996) 45.
- [3] Economos G., *J. Am. Ceram. Society*, 1955, vol 38, p. 241.
- [4] G Albanese., *J. De Physique*, Apr. 1977, suppl 4, vol 38, p. C1-85.
- [5] E.W. Gorter, *Magnetism, materials and applications*, proceedings of IEE (London), 1957, vol. 104B, suppl 5, p. 255.
- [6] K. Kouril, V. Chlan, H. Stepankova, A. Telfah, P. Novak. K. Knizek, Y. Hiraoka and T. Kimura, *Acta Physica Polonica A*, 2010 vol. 118, P732.
- [7] D. B. Ghare, Sinha A. B. P., *Phys. Chem. Solids*, 1968, vol. 29, p. 885.
- [8] Y. Bai, J. Z. Gui, L. Li, *Mater Chem Phys* 2006, vol. 98(1), p. 66-70.
- [9] K. Handea and H. Kojima, *J. Phys. Status Solidi* 1971, vol (A) 6, p. 259.
- [10] V.R.K. Murthy, S. Sundaram, and B. Vishwanathan, *Microwave Materials*, Narosa publishing House, New Delhi, 1993.
- [11] A. ghasemi, A. Hossienpour, A. Morisako, A. Saatchi and M. Salehi, *J. Magn. Mater.* 2006, vol. 302, p. 429.
- [12] C. Wang, L. Li. J. Zhou, X. Qi, and Z. Yue, *J. Mater. Sci. : Mater. Electron.* 2002, vol. 13, p. 713.
- [13] H. S. Cho and S. S. Kim, *IEEE Trans. Magn.* 1999, vol. 35, p. 3151.

ISSN 2229-5518

- [14] S. Sugimoto, S. Kondo, K.Okayama, H. Nakamura, D. Book, T. Kagotani, M. Homma, H. Ota, M. Kimura, and R. Sato, *IEEE Trans. Magn.* 199, vol. 35, p.3154
- [15] Jander, *Phys. Rev.*, 1928, vol. 6, p. 596.
- [16] Ghare D. B., and Sinha A. P. *J. phys. Chem. Solids*, 1968, vol. 29, p. 885
- [17] Kshirsagar S. T., *J. Phy. Soc. Japan*, 1969, vol. 25 (5), p. 164.
- [18] Standley K. J., *Oxides Magnetic Materials* (Oxford Uni. Press), 1972.
- [19] Van Uitert L. G., *J. Appl. Phys.*, 1957, vol. 28, p. 317
- [20] Sabane C. D., Sinha A. P. B., and Biswas A. B., *Indian J. Pure and App. Phys.*, 1966, vol. 4, p. 187.
- [21] Bates L. F., *Modern Magnetism*, (Cambridge Uni. Press) 1939.
- [22] Kohn J. A., and Kchart D. W., *J. Appl. Phys.* 1964 vol. 35, p. 968.
- [23] Braun P. B., *Philips research repts*, 1957, vol. 12, p. 491
- [24] Smit J. and Wijn H. P. J., *Ferrites*, John Wiley and Sons, Inc, New York, (1959)
- [25] Tsang-Tse-Fang, Hwang J. B., and Shiau F. S., *J. Mat. Sci. Lett.*, 1992, vol. 11, p. 1217
- [26] Sailakshmi K., B. Ramesh, A. D. P. Rao and Raju S. B., *J. Magnetism Soc. of Japan*, 1998, vol. 22 (S1), p. 37

IJSER